Spectral microscopic mechanisms and quantum phase transitions in a 1D correlated problem



2006 J. Phys.: Condens. Matter 18 2881

(http://iopscience.iop.org/0953-8984/18/10/011)

INSTITUTE OF PHYSICS PUBLISHING JOURNAL OF PHYSICS: CONDENSED MATTER

J. Phys.: Condens. Matter **18** (2006) 2881–2895 doi:10.1088/0953-8984/18/10/011

# Spectral microscopic mechanisms and quantum phase transitions in a 1D correlated problem

**J M P Carmelo**[1,2] **and K Penc**[3]

[1] Department of Physics, Massachusetts Institute of Technology, Cambridge, MA 02139-4307, USA
[2] GCEP—Center of Physics, University of Minho, Campus Gualtar, P-4710-057 Braga, Portugal
[3] Research Institute for Solid State Physics and Optics, H-1525 Budapest, PO Box 49, Hungary

Received 9 August 2005
Published 20 February 2006
Online at stacks.iop.org/JPhysCM/18/2881

**Abstract**

In this paper we study the dominant microscopic processes that generate nearly the whole one-electron removal and addition spectral weight of the one-dimensional Hubbard model for all values of the on-site repulsion $U$. We find that for the doped Mott–Hubbard insulator there is a competition between the microscopic processes that generate the one-electron upper-Hubbard-band spectral-weight distributions of the Mott–Hubbard insulating phase and finite-doping-concentration metallic phase, respectively. The spectral-weight distributions generated by the non-perturbative processes studied here are shown elsewhere to agree quantitatively for the whole momentum and energy bandwidth with the peak dispersions observed by angle-resolved photoelectron spectroscopy in quasi-one-dimensional compounds.

## 1. Introduction

For energies larger than the transfer integrals for electronic hopping between the chains, the one-dimensional (1D) Hubbard Hamiltonian is the simplest model for the description of electronic correlation effects on the spectral properties of quasi-1D compounds [1–4]. It reads

$$\hat{H} = -t \sum_{j,\sigma} [c^{\dagger}_{j,\sigma} c_{j+1,\sigma} + \text{h.c.}] + U \sum_{j} \hat{n}_{j,\uparrow} \hat{n}_{j,\downarrow}, \tag{1}$$

where $c^{\dagger}_{j,\sigma}$ and $c_{j,\sigma}$ are spin-projection $\sigma = \uparrow, \downarrow$ electron operators at site $j = 1, 2, \ldots, N_a$, $\hat{n}_{j,\sigma} = c^{\dagger}_{j,\sigma} c_{j,\sigma}$, and $t$ is the transfer integral. In contrast to other interacting models [5] and in spite of the model exact solution [6, 7], for finite values of the on-site repulsion $U$ little is known about the non-perturbative microscopic processes that control its finite-energy spectral properties. Recently, the problem was studied in [8, 9] by the use of a pseudofermion description. The preliminary predictions of the method introduced in these references agree quantitatively for the whole momentum and energy bandwidth with the peak dispersions

observed by angle-resolved photoelectron spectroscopy in the quasi-1D conductor TTF-TCNQ [1, 2] and are consistent with the phase diagram of the $(TMTTF)_2X$ and $(TMTSF)_2X$ series of compounds [4]. More recently, results for the TTF-TCNQ spectrum consistent with those of [1, 2] were obtained by the dynamical density matrix renormalization group method [3]. Within the method of [8, 9], the finite-energy spectral properties are controlled by the overall pseudofermion phase shifts, through the pseudofermion anticommutators [10]. Such a method is a generalization for all values of the on-site repulsion $U$ of the technique introduced in [11, 12] for $U \rightarrow \infty$.

The studies of this paper focus on the specific case of the one-electron spectral weight and use the pseudofermion description used in the general studies of [8]. Such a description is related to the holon, spinon, and $c$ pseudoparticle representation introduced in [13]. Here we study the generators of the one-electron dominant microscopic processes and the interplay between such processes and the metal–Mott–Hubbard insulator quantum phase transition [14]. Since the mechanisms found here are expected to occur in other correlated models, our results are of interest for the further general understanding of the microscopic mechanisms associated with the quantum phase transitions. Furthermore, they are of interest for the further understanding of the unusual spectral properties observed in low-dimensional materials.

The model (1) describes $N_\uparrow$ spin-up electrons and $N_\downarrow$ spin-down electrons in a chain of $N_a$ sites. We denote the electronic number by $N = N_\uparrow + N_\downarrow$. The number of lattice sites $N_a$ is even and very large. For simplicity, we use units such that both the lattice spacing $a$ and the Planck constant are unity. In these units the chain length $L$ is such that $L = N_a a = N_a$. Our results refer to periodic boundary conditions. We consider an electronic density $n = n_\uparrow + n_\downarrow$ in the range $0 < n \leqslant 1$ and a spin density $m = n_\uparrow - n_\downarrow = 0$, where $n_\sigma = N_\sigma/L$ and $\sigma = \uparrow, \downarrow$. We introduce the Fermi momenta which, in the thermodynamic limit $L \rightarrow \infty$, are given by $\pm k_{F\sigma} = \pm\pi n_\sigma$ and $\pm k_F = \pm[k_{F\uparrow} + k_{F\downarrow}]/2 = \pm\pi n/2$. The one-electron spectral function $B^l(k,\omega)$ such that $l = -1$ (and $l = +1$) for electron removal (and addition), is given by

$$
\begin{aligned}
B^{-1}(k,\omega) &= \sum_\sigma \sum_f |\langle f|c_{k,\sigma}|GS\rangle|^2 \delta\big(\omega + E_{f,N-1} - E_{GS}\big), \qquad \omega < 0; \\
B^{+1}(k,\omega) &= \sum_\sigma \sum_{f'} |\langle f'|c^\dagger_{k,\sigma}|GS\rangle|^2 \delta\big(\omega - E_{f',N+1} + E_{GS}\big), \qquad \omega > 0.
\end{aligned}
\tag{2}
$$

Here $c_{k,\sigma}$ (and $c^\dagger_{k,\sigma}$) are electron annihilation (and creation) operators of momentum $k$ and $|GS\rangle$ denotes the initial $N$-electron ground state. The $f$ and $f'$ summations run over the $N-1$ and $N+1$-electron excited states, respectively, and $[E_{f,N-1} - E_{GS}]$ and $[E_{f',N+1} - E_{GS}]$ are the corresponding excitation energies.

The Hamiltonian (1) commutes with the generators of the $\eta$-spin and spin $SU(2)$ algebras [13, 15, 16]. Here we call the $\eta$-spin and spin of the energy-eigenstates $\eta$ and $S$, respectively, and the corresponding projections $\eta_z$ and $S_z$. All such states can be described in terms of occupancy configurations of $\eta$-spin $1/2$ holons, spin $1/2$ spinons, and $\eta$-spinless and spin-less $c0$ pseudoparticles [13]. (The latter objects are called $c$ pseudoparticles in [13, 17].) We use the notation $\pm 1/2$ holons and $\pm 1/2$ spinons according to the values of the $\eta$-spin and spin projections, respectively. For large values of $U/t$ the $+1/2$ holons and $-1/2$ holons become the holons and doublons, respectively, used in the studies of [18]. The electron–rotated-electron unitary transformation [13] maps the electrons onto rotated electrons such that rotated-electron double occupation, unoccupancy, and spin-up and spin-down single occupation are good quantum numbers for all values of $U$. While the $-1/2$ and $+1/2$ holons refer to the rotated-electron doubly occupied and unoccupied sites, respectively, the $-1/2$ and $+1/2$ spinons correspond to the spin degrees of freedom of the spin-down and spin-up rotated-electron singly occupied sites, respectively. The charge degrees of freedom of the latter sites are

described by the spin-less and $\eta$-spin-less $c0$ pseudoparticles. In turn, the $c\nu$ pseudoparticles (and $s\nu$ pseudoparticles) such that $\nu = 1, 2, \ldots$ are $\eta$-spin singlet (and spin singlet) $2\nu$-holon (and $2\nu$-spinon) composite objects. Thus, the numbers of $\pm 1/2$ holons ($\alpha = c$) and $\pm 1/2$ spinons ($\alpha = s$) read $M_{\alpha,\pm 1/2} = L_{\alpha,\pm 1/2} + \sum_{\nu=1}^{\infty} \nu N_{\alpha\nu}$, where $\alpha = c, s$, $N_{\alpha\nu}$ denotes the number of $\alpha\nu$ pseudoparticles, and $L_{c,\pm 1/2} = [\eta \mp \eta_z]$ and $L_{s,\pm 1/2} = [S \mp S_z]$ gives the number of $\pm 1/2$ Yang holons and $\pm 1/2$ HL spinons, respectively. These are the holons and spinons that are not part of composite pseudoparticles. The total number of holons ($\alpha = c$) and spinons ($\alpha = s$) is given by $M_\alpha = [M_{\alpha,+1/2} + M_{\alpha,-1/2}]$.

The $c0$ pseudofermions and composite pseudofermions are generated from the $c0$ pseudoparticles and composite pseudoparticles of [13] by a unitary transformation [8]. It introduces shifts of order $1/L$ in the pseudoparticle discrete momentum values and leaves all other pseudoparticle properties invariant. It is useful for our study to consider the pseudofermion subspace (PS), which is spanned by the initial ground state $|GS\rangle$ and all excited energy eigenstates contained in the one-electron excitations $c^\dagger_{j,\sigma}|GS\rangle$ and $c_{j,\sigma}|GS\rangle$ [8]. The local $\alpha\nu$ pseudofermion creation (and annihilation) operator $f^\dagger_{x_j,\alpha\nu}$ (and $f_{x_j,\alpha\nu}$) creates (and annihilates) a $\alpha\nu$ pseudofermion at the effective $\alpha\nu$ lattice site of spatial coordinate $x_j = j a^0_{\alpha\nu}$. Here $j = 1, 2, \ldots, N^*_{\alpha\nu}$ and $a^0_{\alpha\nu} = 1/n^*_{\alpha\nu}$ is the effective $\alpha\nu$ lattice constant given in equation (55) of [17] in units of the electronic lattice constant and $n^*_{\alpha\nu} = N^*_{\alpha\nu}/L = N^*_{\alpha\nu}/N_a$. The general expression of the number of effective $\alpha\nu$ lattice sites $N^*_{\alpha\nu}$ is given in equation (B6) of [13], where the number of $\alpha\nu$ pseudofermion holes $N^h_{\alpha\nu}$ is provided in equation (B.11) of the same reference. All PS energy eigenstates can be described by occupancy configurations of $\alpha\nu$ pseudofermions, $-1/2$ Yang holons, and $-1/2$ HL spinons [13]. For the ground state, $N_{c0} = N, N_{s1} = N_\downarrow$, and $N_{c\nu} = N_{s\nu'} = L_{\alpha,-1/2} = 0$ for $\alpha = c, s$, $\nu > 0$, and $\nu' > 1$. The deviations $\Delta N_{\alpha\nu}$, $\Delta N^h_{\alpha\nu}$, $\Delta L_{c,-1/2}$, $\Delta L_{s,-1/2}$, $\Delta M_{c,-1/2}$, $\Delta M_{s,-1/2}$, $\Delta M_c$, $\Delta M_s$ of the above numbers which result from the ground-state–excited-energy-eigenstate transitions play a major role in our study. It follows from the values of the ground-state numbers that $\Delta N_{c\nu} = N_{c\nu}$, $\Delta N_{s\nu'} = N_{s\nu'}$, $\Delta L_{c,-1/2} = L_{c,-1/2}$, $\Delta L_{s,-1/2} = L_{s,-1/2}$, $\Delta M_{c,-1/2} = M_{c,-1/2}$, and $\Delta M_{s,-1/2} = M_{s,-1/2}$ for $\nu > 0$ and $\nu' > 1$. Thus, often we replace the latter deviations by the corresponding numbers. A concept widely used in our studies is that of a CPHS ensemble subspace [8, 9]. (Here CPHS stands for $c0$ pseudofermion, holon, and spinon.) Such a subspace is spanned by all energy eigenstates with fixed values for the $-1/2$ Yang holon number $L_{c,-1/2}$, $-1/2$ HL spinon number $L_{s,-1/2}$, and for the sets of $\alpha\nu$ pseudofermion numbers $\{N_{c\nu}\}$ and $\{N_{s\nu'}\}$ corresponding to the $\nu = 0, 1, 2, \ldots$ and $\nu' = 1, 2, \ldots$ branches. Fortunately, nearly the whole one-electron weight corresponds to subspaces involving the $c0$, $c1$, $s1$, and $s2$ branches only.

For the ($\mathcal{N} = 1$)-electron problem, the operator $\hat{O}^l_{\mathcal{N},j} = \hat{O}^l_{1,j}$ of the spectral-function expressions of equation (7) of [9] is the operator $c_{j,\sigma}$ for $l = -1$ and $c^\dagger_{j,\sigma}$ for $l = +1$. These expressions can be re-expressed in terms of the operator $\hat{\Theta}^l_{\mathcal{N},j}$, which plays an important role in our study and is defined in terms of the original $\mathcal{N}$-electron operator $\hat{O}^l_{\mathcal{N},j}$ in equations (27) and (28) of [9]. For the present $\mathcal{N} = 1$ problem we use the notations $\hat{\theta}_{j,\sigma}$ and $\hat{\theta}^\dagger_{j,\sigma}$ for the operators $\hat{\Theta}^{-1}_{1,j}$ and $\hat{\Theta}^{+1}_{1,j}$, respectively, and call $\tilde{\theta}_{i,j,\sigma}$ and $\tilde{\theta}^\dagger_{i,j,\sigma}$ the operators $\tilde{\Theta}^{-1}_{1_i,j}$ and $\tilde{\Theta}^{+1}_{1_i,j}$, respectively, on the right-hand side of equation (32) of [9]. The latter equation then reads

$$\hat{\theta}_{j,\sigma} = \tilde{\theta}_{0,j,\sigma} + \sum_{i=1}^{\infty} \sqrt{c_i^{-1}}\,\tilde{\theta}_{i,j,\sigma}; \qquad j = 1, 2, \ldots, N_a; \quad l = \pm 1, \tag{3}$$

and a similar expression with $c_i^{-1}$ replaced by $c_i^{+1}$ holds for $\hat{\theta}^\dagger_{j,\sigma}$, where for $i > 0$ the index $i = 1, 2, \ldots$ is a positive integer number which increases for increasing values of the number

of extra pairs of creation and annihilation rotated-electron operators in the expressions of the operators $\tilde{\theta}_{i,j,\sigma}$ relative to that of $\tilde{\theta}_{0,j,\sigma}$, and the value of the constants $c_i^{\pm 1}$ reads $c_0^{\pm 1} = 1$ and for $i > 0$ is a function of $n$, $m$, and $U/t$ such that $c_i^{\pm 1} \rightarrow 0$ as $U/t \rightarrow \infty$ [9]. Moreover, the operators $\hat{\theta}_{j,\sigma}$ and $\tilde{\theta}_{0,j,\sigma}$ of equation (3) have the same expression in terms of local creation and annihilation electron and rotated-electron operators, respectively.

According to the general studies of [8, 9], the $i = 0$ operators $\tilde{\theta}^{\dagger}_{0,j,\sigma}$ and $\tilde{\theta}_{0,j,\sigma}$ generate nearly the whole spectral weight of the corresponding one-electron problems for all values of $U/t$ and $L \rightarrow \infty$. In the ensuing section we confirm numerically that the same occurs for finite values of the chain length $L$ and treat the problem analytically for $L \rightarrow \infty$ and large values of $U/t$. Since the physics associated with the dominant microscopic processes that control the one-electron weight distribution is simplest when understood in terms of pseudofermion occupancies, in section 3 we calculate the expressions of the above operators in terms of local pseudofermion operators. In section 4 we study the main microscopic effects of the metal–Mott–Hubbard insulator quantum phase transition onto the one-electron spectral properties. Finally, the concluding remarks are presented in section 5.

## 2. One-electron spectral-weight dominant processes

Application to the ground state of the operators $\tilde{\theta}^{\dagger}_{0,j,\sigma}$ or $\tilde{\theta}_{0,j,\sigma}$ generates transitions to excited energy eigenstates whose $M_{c,-1/2} = L_{c,-1/2} + \sum_{\nu=1}^{\infty} \nu N_{c\nu}$ values obey the following exact charge selection rule [9]:

$$M_{c,-1/2} = 0, \quad \text{electron removal;} \qquad M_{c,-1/2} = 0, 1, \quad \text{electron addition,} \tag{4}$$

where *electron* refers here to a rotated electron. Thus, in the present case we only need to consider excited states such that $L_{c,-1/2} \leqslant 1$ and $N_{c\nu} = 0$ for $\nu > 1$. Moreover, the values of the numbers of $-1/2$ HL spinons generated by application to the ground state of the operators $c^{\dagger}_{j,\sigma}$ and $c_{j,\sigma}$ are restricted to the following ranges:

$$\begin{aligned} L_{s,-1/2} &= 0, \quad \downarrow \text{electron removal}, \quad \uparrow \text{electron addition} \\ &= 0, 1, \quad \downarrow \text{electron addition}, \quad \uparrow \text{electron removal}, \end{aligned} \tag{5}$$

whereas the permitted values of $L_{c,-1/2}$ coincide with those of equation (4).

While the selection rules (4) and (5) are exact for the one-rotated-electron and one-electron problems, respectively, direct evaluation of the weights by the method introduced of [8, 9] reveals that for $\mathcal{N}_0 = 1$ 94%–98% of the spectral weight generated by the operators $\tilde{\theta}^{\dagger}_{0,j,\sigma}$ or $\tilde{\theta}_{0,j,\sigma}$ corresponds to transitions to excited energy eigenstates whose $L_{s,-1/2}$ and $N_{s\nu}$ values for $\nu > 1$ are in the following range:

$$\begin{aligned} L_{s,-1/2} + \sum_{\nu=2}^{\infty} (\nu - 1) N_{s\nu} &= 0, \quad \downarrow \text{electron removal}, \quad \uparrow \text{electron addition} \\ &= 0, 1, \quad \downarrow \text{electron addition}, \quad \uparrow \text{electron removal}, \end{aligned} \tag{6}$$

where *electron* refers here to rotated electron. Thus, in the present case most of the spectral weight corresponds to excited states such that $L_{s,-1/2} \leqslant 1$ and $N_{s\nu} = 0$ for $\nu > 2$.

One-electron processes associated with excited energy eigenstates whose deviations do not obey the rule (4) are generated by the operators $\tilde{\theta}_{i,j,\sigma}$ or $\tilde{\theta}^{\dagger}_{i,j,\sigma}$ such that $i > 0$. We confirm below that application to the ground state of all such $i > 0$ operators amounts for less than 1% of the $(k, \omega)$-plane one-electron removal or addition spectral weight. We start by confirming that the one-electron processes which generate excited energy eigenstates obeying the ground-state charge selection rule (4) are dominant for finite values of $L$ and correspond

to 99.75%–100.00% of the whole electronic spectral weight for all values of $U/t$. For finite values of $L$ the thermodynamic Bethe-ansatz equations introduced by Takahashi [7] do not apply, whereas the Bethe-ansatz solution and the concept of a rotated electron remain valid. Therefore, for finite values of $L$ we can characterize the excited energy eigenstates in terms of rotated-electron occupancy configurations and thus of the related $\pm 1/2$ holon, $\pm 1/2$ spinon, and $c0$ pseudofermion number deviations [17]. Moreover, for zero-magnetization initial ground states the number of excited-energy-eigenstate $s1$ pseudofermion holes equals the number of holes in the corresponding Bethe-ansatz spin excitation spectrum. Thus, one can classify the finite-$L$ processes by the deviation values $\Delta N_{c0}$, $M_{c,-1/2}$, $\Delta M_{s,-1/2}$, $\Delta M_c$, $\Delta M_s$, and $\Delta N^h_{s1}$.

The correlation energy $2\mu$, defined in equation (21) of [8], plays an important role in the model finite-energy spectrum. The limiting value of such a correlation energy is given in equation (13) of [9]. At half filling it equals the Mott–Hubbard gap, $2\mu = E_{\rm MH}$. Our considerations refer mostly to one-electron addition. For simplicity, let us assume that the initial ground state has zero spin density. In this case the spectral-weight distribution associated with creation of a spin-up electron has the same form as that associated with creation of a spin-down electron. Here we consider the former case. For creation of a spin-up rotated electron, the selection rule (4) only allows the two values $\Delta M_{c,-1/2} = M_{c,-1/2} = 0, 1$. From the relation of the electron and rotated-electron numbers to the holon, spinon, and $c0$ pseudofermion numbers [13, 17], we find that for creation of a spin-up rotated electron the following transitions obey the selection rule (4):

(i) Lower-Hubbard-band (LHB) transitions such that $\Delta N_{c0} = 1$, $\Delta M_{c,-1/2} = 0$, $\Delta M_{s,-1/2} = 0$, $\Delta M_c = -1$, and $\Delta M_s = 1$. The minimal excitation energy for such transitions is zero. The sub-class of these transitions that also obey the restrictions of equation (6) is such that $\Delta N^h_{s1} = 1$.

(ii) Upper-Hubbard-band (UHB) transitions such that $\Delta N_{c0} = -1$, $\Delta M_{c,-1/2} = 1$, $\Delta M_{s,-1/2} = -1$, $\Delta M_c = 1$, and $\Delta M_s = -1$. The minimal excitation energy for such transitions is $2\mu$. The sub-class of these transitions that also obey the restrictions of equation (6) correspond to an $s1$ pseudofermion-hole deviation value $\Delta N^h_{s1} = 1$.
The simplest transitions that do not obey the selection rule (4) involve creation of three $c0$ pseudofermion holes and three holons, as follows.

(iii) Second-UHB transitions such that $\Delta N_{c0} = -3$, $\Delta M_{c,-1/2} = 2$, $\Delta M_{s,-1/2} = -2$, $\Delta M_c = 3$, and $\Delta M_s = -3$. The minimal excitation energy for such transitions is $4\mu$. The sub-class of these transitions that also obey the restrictions of equation (6) is such that $\Delta N^h_{s1} = 1$. The simplest transitions of types (i) and (ii) that do not obey the restrictions (6) involve creation of three $s1$ pseudofermion holes:

(i′) and (ii′) transitions with the same values for the deviations $\Delta N_{c0}$, $\Delta M_{c,-1/2}$, $\Delta M_{s,-1/2}$, $\Delta M_c$, $\Delta M_s$ as for the above general (i) and (ii) transitions, respectively, and $\Delta N^h_{s1} = 3$. The minimal excitation energy for such transitions is zero and $2\mu$, respectively.

For the Mott–Hubbard insulator quantum phase such that $n = 1$ one often shifts the ground-state zero-energy level to the middle of the Mott–Hubbard gap. Then the excitation energies 0, $E_{\rm MH}$, and $2E_{\rm MH}$ become 0, $E_{\rm MH}/2$, and $3E_{\rm MH}/2$, respectively. Here we call the excited energy eigenstates of the transitions (iii) *three-holon states*, because these involve the creation of three holons. Such excited energy eigenstates also involve the annihilation of three $c0$ pseudofermions. Moreover, we call the excited energy eigenstates of transitions (i′) and (ii′) *three-s1-hole states*. These involve creation of three $s1$ pseudofermion holes. Finally, LHB and UHB excited energy eigenstates belonging to the sub-class of the general states generated by both the transitions (i) and (ii) such that $\Delta N^h_{s1} = 1$ are called one-holon and one-$s1$-hole states.

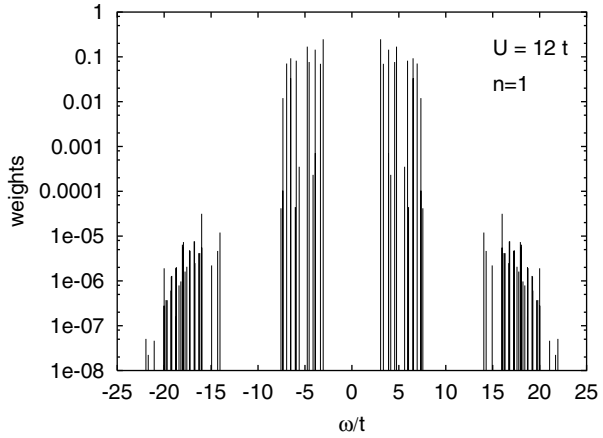


**Figure 1.** Electron addition ($\omega > 0$) and removal ($\omega < 0$) spectrum for a half-filled finite-site ring, with $U = 12t$. Note the logarithmic scale for the weights. The five-holon states are not shown. Indeed, the contributions of these states are extremely small and their energies are out of the shown energy window.

We start by evaluating the relative weight of the excited states of type (iii) (or states of types (iii), (i′), and (ii′)) relative to the weight of the states of types (i) and (ii) (or states of types (i) and (ii) such that $\Delta N^h_{s1} = 1$) when all these states are generated by application to the ground state of the spin-up electron creation operator. (The types of excited energy eigenstate refer to the above transitions which generate these states from the ground state.) To assess the importance for finite values of $L$ of the three-holon final states of type (iii) and three-$s1$-hole states of types (i′) and (ii′), we perform an exact diagonalization of small chains. There is no one-to-one correspondence between the small-chain weight associated with each specific excited energy eigenstate and the excited-energy-eigenstate weight for $L \rightarrow \infty$. However, there is such a correspondence for the spectral-weight sum rules of the states of types (i) and (ii) generated by dominant processes, relative to the sum rule of the states of type (iii). Moreover, within the excited energy eigenstates generated by dominant processes, we consider the relative weight of the states of types (i′) and (ii′). For these spectral-weight sum rules the small-chain results provide values for the relative weights which agree up to 99% with the corresponding thermodynamic-limit values.

The full electron addition and removal spectrum for six sites with six electrons (half filling) is shown in figure 1 for $U = 12t$. (We checked that similar results are obtained for larger finite systems.) The first Hubbard bands at $\pm E_{\rm MH}/2$ are generated by dominant processes, whereas the second Hubbard bands at $+3E_{\rm MH}/2$ and $-3E_{\rm MH}/2$ result from processes generated by the above $i > 0$ operators $\tilde{\theta}^{\dagger}_{i,j,\sigma}$ and $\tilde{\theta}_{i,j,\sigma}$, respectively. Note that the first and second Hubbard bands are well separated. The weights of the latter bands are orders of magnitude smaller than the contribution from the first Hubbard bands. The states centred around $3E_{\rm MH}/2$ are three-holon states of type (iii). As a result of the half-filling particle–hole symmetry, there is a corresponding structure for electron removal centred around $-3E_{\rm MH}/2$. The latter structure is associated with creation of two rotated-electron unoccupied sites. (We recall that the $-1/2$ holon number deviation selection rule (4) refers to excited-energy-eigenstate electronic densities such that $n < 1$. There is a corresponding $+1/2$ holon number deviation selection rule for $n > 1$.)

In figure 2 we plot the contribution of different excited energy eigenstates to the sum rule for half filling. For this, we have followed adiabatically the weights of different states as the

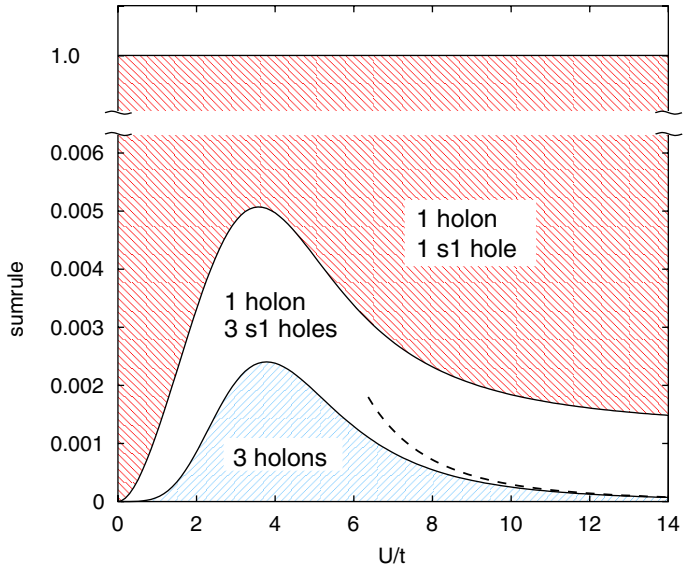


**Figure 2.** The contribution of different states to the electron-addition sum rule for half filling. Over 99% of the sum rule is exhausted by one-holon and one-$s1$ pseudofermion hole excited energy eigenstates of type (ii). For larger systems this remains true if we also consider the states of type (ii′), which like the states of type (ii) are also associated with dominant processes generated by the $i = 0$ operator $\tilde{\theta}^{\dagger}_{0,j,\sigma}$.

(This figure is in colour only in the electronic version)

value of $U/t$ is reduced, and summed the weight over the particular family of states. Analysis of the figure reveals that the contribution of the three-holon excited energy eigenstates of type (iii) to the total sum rule is largest at intermediate values $U \approx 4t$. It does not exceed 0.25% in the total sum rule. For large values of $U/t$ it decreases as $(t/U)^4$, while for small values as $(U/t)^4$. The three-$s1$-hole contribution of the above states of type (ii′) is also less than 0.25%, and for small values of $U/t$ it decreases as $(U/t)^2$. (These states belong to a sub-class of the excited energy eigenstates of type (ii).) While figure 2 corresponds to $n = 1$, the relative spectral weight of the excited energy eigenstates of type (iii) decreases for decreasing values of the electronic density $n$. For instance, at quarter filling such a weight is 2% of that of half filling and vanishes as $n \to 0$. Thus, at quarter filling and $U \approx 4t$ the excited energy eigenstates of types (i) and (ii) (including the states of types (i′) and (ii′)) correspond to ≈99.99% of the total spectral weight and the states (iii) to ≈0.005% of such a weight.

Evaluation for the model metallic phase of the available spectral-weight contributions by the method of [8, 9] confirms that the above results remain valid for $L \to \infty$. The exception is the relative weight of the excited energy eigenstates of types (i′) and (ii′), which increases for increasing values of $L$. This is confirmed by the values given in table 1, which displays the relative weights generated by the transitions to the one-$s1$-pseudfermion-hole excited energy eigenstates that obey the relation (6) both for the one-electron removal and addition spectral functions. These weights were obtained for the one-electron spectral functions as $U/t \to \infty$. For $L \to \infty$ and $U/t \to \infty$ the use of the method of [12] leads to values of the relative weights for one-electron removal and addition of approximately 98% and 94%, respectively. On the other hand, the set of excited energy eigenstates which obey the exact selection rule (4) is larger: it corresponds to the whole one-rotated-electron spectral weight. The excited energy

**Table 1.** The relative weight of the one-$s$1-pseudfermion hole contributions that obey relation (6) in the $U/t \rightarrow \infty$ limit for finite-size systems of $N$ electrons.

| $N$ | Electron removal | Electron addition |
|---|---|---|
| 6 | 0.998 792 | 0.977 515 |
| 8 | 0.997 486 | 0.972 141 |
| 10 | 0.996 277 | 0.968 088 |
| 12 | 0.995 178 | 0.964 847 |
| 14 | 0.994 176 | 0.962 156 |
| 16 | 0.993 258 | 0.959 862 |
| 18 | 0.992 409 | 0.957 867 |
| 20 | 0.991 622 | 0.956 105 |
| 22 | 0.990 886 | 0.954 531 |
| 24 | 0.990 196 | 0.953 109 |

eigenstates of types (i′) and (ii′) are associated with dominant processes generated by the $i = 0$ operator $\tilde{\theta}^{\dagger}_{0,j,\sigma}$. In contrast, the states of type (iii) are not generated by dominant processes and remain having very little spectral weight as $L \rightarrow \infty$.

Let us next consider the limit of large $U/t$, where the $L \rightarrow \infty$ problem can be handled analytically by the method of [12]. In that case the general $c0$ pseudofermions of [8, 9] become the spin-less fermions used in the studies of [11, 12]. Our first goal is the confirmation that the contribution from the three-holon states of type (iii) is very small and leads nearly to the same relative weight both for $L \rightarrow \infty$ and finite values of $L$. For large values of $U/t$ one can derive a systematic $t/U$ expansion for the electron–rotated-electron unitary operator defined by equations (21)–(23) of [13]. (See [19], which studies that transformation for large values of $U/t$.) By use of the inverse of the relation between the one-electron and one-rotated-electron operators given in equation (19) of [13] in such a $t/U$ expansion, we find after some algebra the following partial sum rule:

$$\int \mathcal{A}^{\rm 2UHB}(\omega)\,{\rm d}\omega = \frac{t^4}{U^4}\left\langle \tfrac{3}{2} - 2\mathbf{S}_0\mathbf{S}_1 - 2\mathbf{S}_1\mathbf{S}_2 - 2\mathbf{S}_0\mathbf{S}_2\right\rangle_{\rm spin} \times \langle \hat{n}_{x_0,c0}\hat{n}_{x_1,c0}\hat{n}_{x_2,c0}\rangle, \tag{7}$$

where $\hat{n}_{x_j,c0} = f^{\dagger}_{x_j,c0}f_{x_j,c0}$. The expectation value $\left\langle \frac{3}{2} - 2\mathbf{S}_0\mathbf{S}_1 - 2\mathbf{S}_1\mathbf{S}_2 - 2\mathbf{S}_0\mathbf{S}_2\right\rangle_{\rm spin}$ refers to the spin degrees of freedom. The partial sum rule (7) corresponds to the second UHB. This band is generated by transitions to the above three-holon states of type (iii) and involves annihilation of three $c0$ pseudofermions. The expectation value to find three neighbouring local $c0$ pseudofermions is

$$\begin{aligned}\langle \hat{n}_{x_0,c0}\hat{n}_{x_1,c0}\hat{n}_{x_2,c0}\rangle &= \begin{vmatrix} \langle f^{\dagger}_{x_0,c0}f_{x_0,c0}\rangle & \langle f^{\dagger}_{x_0,c0}f_{x_1,c0}\rangle & \langle f^{\dagger}_{x_0,c0}f_{x_2,c0}\rangle \\ \langle f^{\dagger}_{x_1,c0}f_{x_0,c0}\rangle & \langle f^{\dagger}_{x_1,c0}f_{x_1,c0}\rangle & \langle f^{\dagger}_{x_1,c0}f_{x_2,c0}\rangle \\ \langle f^{\dagger}_{x_2,c0}f_{x_0,c0}\rangle & \langle f^{\dagger}_{x_2,c0}f_{x_1,c0}\rangle & \langle f^{\dagger}_{x_2,c0}f_{x_2,c0}\rangle \end{vmatrix} \\ &= n^3 - \frac{2n\sin^2(\pi n)}{\pi^2} + \frac{\sin^2(\pi n)\sin(2\pi n)}{\pi^3} \\ &\quad - \frac{n\sin^2(2\pi n)}{4\pi^2}. \end{aligned} \tag{8}$$

This expectation value has the following limiting behaviour:

$$\langle \hat{n}_{x_0,c0}\,\hat{n}_{x_1,c0}\,\hat{n}_{x_2,c0}\rangle = \begin{cases} \dfrac{4\pi^6}{135}n^9 & \text{if } n \ll 1; \\ 1 - 3(1-n) & \text{if } 1-n \ll 1. \end{cases} \tag{9}$$

Note that the spectral weight generated by the transitions to the three-holon states of type (iii) decreases rapidly away from half filling. At quarter filling ($n = 1/2$) it is about 2% of that at half filling.

The expectation values associated with the spin degrees of freedom can in the thermodynamic limit and for large values of $U/t$ be evaluated by use of the relation between the 1D Hubbard model and the spin 1/2 isotropic Heisenberg chain [11, 12]. This leads to the following values [20]:

$$\langle \mathbf{S}_0 \mathbf{S}_1 \rangle_{\rm spin} = \tfrac{1}{4} - \ln 2 \approx -0.443\ 147 \tag{10}$$

$$\langle \mathbf{S}_0 \mathbf{S}_2 \rangle_{\rm spin} = \tfrac{1}{4} - 4\ln 2 + \tfrac{9}{4}\zeta(3) \approx 0.182\ 039, \tag{11}$$

so that

$$\left\langle \tfrac{3}{2} - 2\mathbf{S}_0\mathbf{S}_1 - 2\mathbf{S}_1\mathbf{S}_2 - 2\mathbf{S}_0\mathbf{S}_2 \right\rangle_{\rm spin} = 12\ln 2 - \tfrac{9}{2}\zeta(3) \approx 2.91. \tag{12}$$

The sum rule of the second UHB is then given by

$$\int \mathcal{A}^{\rm 2UHB}(\omega)\, {\rm d}\omega \approx 2.91 \frac{t^4}{U^4} \langle \hat{n}_{x_0,c0} \hat{n}_{x_1,c0} \hat{n}_{x_2,c0} \rangle. \tag{13}$$

For the six-site finite-size cluster, the expectation value (12) is

$$\left\langle \tfrac{3}{2} - 2\mathbf{S}_0\mathbf{S}_1 - 2\mathbf{S}_1\mathbf{S}_2 - 2\mathbf{S}_0\mathbf{S}_2 \right\rangle_{\rm spin} = (169 + 17\sqrt{13})/78 \approx 2.95, \tag{14}$$

which is about 1% off from the thermodynamic-limit value given in equation (12). The asymptotic behaviour $2.95t^4/U^4$ is shown in figure 2 as a dashed line.

Our above numerical results for all values of $U/t$ and a small system lead to the same general picture as the results for $L \rightarrow \infty$. For electron addition the relative spectral weight of the excited energy eigenstates of types (i) and (ii) generated by dominant processes is minimum for $U \approx 4t$. This *minimum* value decreases with decreasing density. For half filling it is given by ≈99.75%, whereas for quarter filling it reads ≈99.99% and in the limit of vanishing density it becomes ≈100.00%. The extremely small amount of missing one-electron addition spectral weight corresponds mainly to the three-holon states of type (iii) generated by the $i > 0$ operators $\tilde{\theta}^{\dagger}_{i,j,\sigma}$. Transitions from the ground state to higher-order five-holon/five-$c$-hole states generated by the latter operators lead to nearly vanishing spectral weight.

The three-$s1$-hole states of types (i′) and (ii′) are generated by a sub-class of dominant processes. The relative weight of these excited energy eigenstates increases for increasing values of the system length $L$. For one-electron addition its maximum value occurs at half filling and is of about 6% as $L \rightarrow \infty$. (At $n = 1$ there are no LHB one-electron addition excited energy eigenstates of types (i) and (i′).) For half filling, all values of $U/t$, and $L \rightarrow \infty$, over 99% of the one-electron addition spectral weight corresponds to generation of one-holon and one- and three-$s1$-pseudofermion holes. This is similar to the relative weights of figure 2 for finite $L$. For $L \rightarrow \infty$ the amount of one-electron spectral weight generated by dominant processes increases for decreasing values of the electronic density for all values of $U/t$.

While for electron addition the states of types (i) and (ii) such that $\Delta N^h_{s1} = 1$ correspond to at least 94% of the spectral weight, for electron removal the $\Delta N^h_{s1} = 1$ excited energy eigenstates amount for at least 98% of the total weight. However, we note that concerning the small amount of spectral weight generated by the excited energy eigenstates such that $\Delta N^h_{s1} > 1$, the case of the 1D Hubbard model is different from that of the $t - J_{XY}$ model considered in [21]. The significant difference is the $SU(2)$ symmetry in the spin sector of the 1D Hubbard model, which by standard selection rules prohibits matrix elements that are present in the $t - J_{XY}$ case. For instance, for low energy such a symmetry *protects* the lower edge of the removal and addition spectrum being dressed by $s1$ pseudofermion particle–hole

excited energy eigenstates in the main conformal tower (see figure 5 in [12]). The low-energy $\Delta N^h_{s1} = 3$ excited energy eigenstates are for the 1D Hubbard model mostly associated with the next conformal tower centred at $3k_F$ for the spin excitations. In the $t - J_{XY}$ case, there is no similar protecting mechanism and, therefore, the weight is more easily redistributed among the $s1$ pseudofermion particle–hole excited energy eigenstates. Let us also note that the studies of [22] have addressed the same question for other models. The authors of that reference found that the weight coming from $\Delta N^h_{s1} = 1$ excited states is also dominant.

## 3. Rotated-electron generators of the one-electron spectral weight

In this section we study the pseudofermion microscopic processes associated with the excitations $c^\dagger_{j,\sigma}|GS\rangle$ and $c_{j,\sigma}|GS\rangle$ which could be expressed in terms of operators of general form given in equation (3). Fortunately, for all values of $U/t$ more than 99% of the spectral weight associated with such excitations corresponds to the $i = 0$ contributions of expression (3). Therefore, here we limit our study to the $i = 0$ operators $\tilde{\theta}^\dagger_{0,j,\sigma}$ and $\tilde{\theta}_{0,j,\sigma}$, which generate nearly the whole one-electron spectral weight measured in photoemission experiments [1, 2]. Indeed, for the electronic densities of the TTF and TCNQ stacks of molecules considered in the photoemission experiments of [2] the studies of the previous section reveal that the dominant processes generated by the operators $\tilde{\theta}^\dagger_{0,j,\sigma}$ and $\tilde{\theta}_{0,j,\sigma}$ account for more than ≈99.9% of the total one-electron spectral weight. We note that in spite of the recent improvements in the resolution of photoemission experiments [2], it is difficult to measure the finest details of the electronic structure experimentally, in part due to the extrinsic losses that occur on very anisotropic conducting solids such as the organic compound TTF-TCNQ [23]. Therefore, the less than 0.01% of missed *theoretical spectral weight* is irrelevant for the description of the spectral features measured by photoemission experiments.

Following the exact selection rule of equation (5) and the corresponding rule for $L_{c,-1/2}$, the CPHS ensemble subspaces of the excited energy eigenstates generated by application of the operators $c^\dagger_{j,\sigma}$ and $c_{j,\sigma}$ onto the ground state can have the following values for the numbers $\{L_{c,-1/2}, L_{s,-1/2}\}$.

$c^\dagger_{j,\downarrow}$ operator: $\{0,0\}, \{1,0\}, \{0,1\}, \{1,1\}$; $c_{j,\downarrow}$ operator: $\{0,0\}$;

$c^\dagger_{j,\uparrow}$ operator: $\{0,0\}, \{1,0\}$; $c_{j,\uparrow}$ operator: $\{0,0\}, \{0,1\}$.

We emphasize that the expressions of the operators $\tilde{\theta}_{0,j,\sigma}$ and $\tilde{\theta}^\dagger_{0,j,\sigma}$ only depend on the values $\{L_{c,-1/2}, L_{s,-1/2}\}$ of the CPHS ensemble subspace they refer to. Different CPHS ensemble subspaces with the same values for $\{L_{c,-1/2}, L_{s,-1/2}\}$ have the same expressions for the operators $\tilde{\theta}_{0,j,\sigma}$ and $\tilde{\theta}^\dagger_{0,j,\sigma}$. Evaluation of the commutators given in equation (27) of [9] for the one-electron case considered here together with the property that the $i = 0$ operators $\tilde{\theta}_{0,j,\sigma}$ and $\tilde{\theta}^\dagger_{0,j,\sigma}$ have the same expressions in terms of rotated-electron creation and annihilation operators as the corresponding operators $\hat{\theta}_{j,\sigma}$ and $\hat{\theta}^\dagger_{j,\sigma}$, respectively, in terms of creation and annihilation electronic operators, leads to the following expressions:

$$
\begin{aligned}
\tilde{\theta}^\dagger_{0,j,\downarrow} &= \tilde{c}^\dagger_{j,\downarrow}, \qquad \{0,0\}, \\
\tilde{\theta}^\dagger_{0,j,\downarrow} &= \frac{(-1)^j}{\sqrt{N_a - N^0 + 1}}\tilde{c}_{j,\uparrow}, \qquad \{1,0\}, \\
\tilde{\theta}^\dagger_{0,j,\downarrow} &= \frac{1}{\sqrt{N^0_\uparrow - N^0_\downarrow + 1}}\tilde{c}^\dagger_{j,\uparrow}, \qquad \{0,1\}, \\
\tilde{\theta}^\dagger_{0,j,\downarrow} &= -\frac{(-1)^j}{\sqrt{(N_a - N^0 + 1)(N^0_\uparrow - N^0_\downarrow + 1)}}\tilde{c}_{j,\downarrow}, \qquad \{1,1\},
\end{aligned}
\tag{15}
$$

and

$$\begin{aligned}
\tilde{\theta}^{\dagger}_{0,j,\uparrow} &= \tilde{c}^{\dagger}_{j,\uparrow}, && \{0,0\},\\
\tilde{\theta}^{\dagger}_{0,j,\uparrow} &= -\frac{(-1)^{j}}{\sqrt{N_a - N^0 + 1}}\tilde{c}_{j,\downarrow}, && \{1,0\},\\
\tilde{\theta}_{0,j,\uparrow} &= \tilde{c}_{j,\uparrow}, && \{0,0\},\\
\tilde{\theta}_{0,j,\uparrow} &= -\frac{1}{\sqrt{N^0_{\uparrow} - N^0_{\downarrow} + 1}}\tilde{c}_{j,\downarrow}, && \{0,1\},\\
\tilde{\theta}_{0,j,\downarrow} &= \tilde{c}_{j,\downarrow}, && \{0,0\},
\end{aligned} \tag{16}$$

where we recall that $0 \leqslant N^0 \leqslant N_a$ and $0 \leqslant N^0_{\downarrow} \leqslant N^0_{\uparrow}$. Here the values of the numbers $\{L_{c,-1/2}, L_{s,-1/2}\}$ are those provided above and $N^0$, $N^0_{\uparrow}$, and $N^0_{\downarrow}$ are the electron numbers of the initial ground state.

The CPHS ensemble subspaces associated with $\eta$-spin value deviations $\Delta\eta$ and spin value deviations $\Delta S$ such that $\Delta\eta = -1/2$ and $\Delta S = -1/2$ are not permitted for initial ground states such that $N^0 = N_a$ and $N^0_{\downarrow} = N^0_{\uparrow}$, respectively. The reason is that for such ground states the $\eta$-spin and spin values are $\eta_0 = 0$ and $S_0 = 0$, respectively, and thus negative deviations $\Delta\eta$ and $\Delta S$ are not allowed. It follows that for $N^0_{\downarrow} = N^0_{\uparrow}$ ground states, the transitions to CPHS ensemble subspaces such that $L_{s,-1/2} = 0$ cannot be generated by application of the operators $c^{\dagger}_{j,\downarrow}$ and $c_{j,\uparrow}$ onto such initial ground states. The case of the $N^0_{\downarrow} = N^0_{\uparrow}$ ground states plays an important role in the applications of our results and those of [8, 9]. In the following, we provide the expression of the operators $\tilde{\theta}_{0,j,\sigma}$ and $\tilde{\theta}^{\dagger}_{0,j,\sigma}$ of equations (15) and (16) in terms of pseudofermion creation and annihilation operators for the set of CPHS ensemble subspaces associated with the $N^0_{\downarrow} = N^0_{\uparrow}$ ground states.

The one-electron processes generated by the rotated-electron operator $\tilde{c}^{\dagger}_{j,\sigma}$ give rise to the LHB when $M_{c,-1/2} = 0$ and UHB when $M_{c,-1/2} = 1$. According to the exact selection rules (4), those are the only permitted values for the excited-energy-eigenstate $-1/2$ holon numbers. Since the numbers of the initial ground-state CPHS subspace are known and well defined, here we characterize the CPHS ensemble subspaces of the excited states associated with the dominant processes by the deviation numbers and numbers $\Delta N_{c0}$, $\Delta N_{s1}$, $N_{s2}$, and $L_{s,-1/2}$. For the UHB we also consider the numbers $N_{c1}$ and $L_{c,-1/2}$. As discussed above, our aim is the study of the dominant microscopic processes that generate the excitations $c^{\dagger}_{j,\uparrow}|GS\rangle$ and $c_{j,\downarrow}|GS\rangle$ where $|GS\rangle$ is a $N^0_{\downarrow} = N^0_{\uparrow}$ ground state.

For simplicity, here and in the ensuing section we consider local generators which are the Fourier transform of the corresponding generators associated with processes such that for each CPHS ensemble subspace all pseudofermion and pseudofermion holes are created away from the *Fermi points* for the $c0$ and $s1$ branches and from the momentum values of largest absolute value for the $s2$ and $c1$ branches. Similar expressions can be derived for processes including creation of pseudofermions or holes at such *Fermi points* and limiting momentum values [8, 9].

The whole $M_{c,-1/2} = 0$ LHB spectral weight of the excitation $\tilde{\theta}^{\dagger}_{0,j,\uparrow}|GS\rangle$ corresponds to $\{L_{c,-1/2}, L_{s,-1/2}\} = \{0,0\}$ CPHS ensemble subspaces. According to equation (16), in such subspaces the above excitation reads $\tilde{\theta}^{\dagger}_{0,j,\uparrow}|GS\rangle = \tilde{c}^{\dagger}_{j,\uparrow}(1 - \tilde{n}_{j,\downarrow})|GS\rangle$ where $(1 - \tilde{n}_{j,\downarrow})$ is the LHB projector. We recall that the LHB processes do not exist for the $N^0 = N_a$ half-filling ground state. Otherwise, the spectral weight of this excitation is generated by transitions to the excited energy eigenstates which span the set of CPHS ensemble subspaces such that

$$\Delta N_{c0} = 1, \qquad \Delta N_{s1} = -2N_{s2}, \qquad N_{s2} = 0, 1. \tag{17}$$

For simplicity, here and in other equations given below we have included only the $\alpha\nu$ branches with finite pseudofermion occupancy for the subset of CPHS ensemble subspaces considered in

our study, which correspond to nearly the whole spectral weight. Thus, the deviation $\Delta N^h_{s1} = \Delta N_{c0} - 2\Delta N_{s1} - 2N_{s2}$ in the number of $s1$ pseudofermion holes is $\Delta N^h_{s1} = -1+2N_{s2}$ for these subspaces. We note that for the present case of zero magnetization the $s1$ pseudofermion band is full for the ground state. Therefore, the deviation $\Delta N^h_{s1}$ equals the number of $s1$ pseudofermion holes of the CPHS ensemble subspace excited energy eigenstates.

At least 94% of the spectral weight of $\tilde{\theta}^{\dagger}_{0,j,\uparrow}|GS\rangle = \tilde{c}^{\dagger}_{j,\uparrow}(1-\tilde{n}_{j,\downarrow})|GS\rangle$ corresponds to the CPHS ensemble subspace such that $\Delta N_{c0} = 1$, $\Delta N_{s1} = 0$, $N_{s2} = 0$, and $\Delta N^h_{s1} = -1$. These numbers obey the relation (6). In this subspace the pseudofermion expression of the operator $\tilde{\theta}^{\dagger}_{0,j,\uparrow} = \tilde{c}^{\dagger}_{j,\uparrow}(1-\tilde{n}_{j,\downarrow})$ is given in equation (47) of [9]. Nearly the whole of the remaining spectral weight of the above LHB excitation is associated with the CPHS ensemble subspace whose numbers are $\Delta N_{c0} = 1$, $\Delta N_{s1} = -2$, $N_{s2} = 1$, and $\Delta N^h_{s1} = 3$. Such values do not obey the relation (6). In this subspace, the pseudofermion expression of the operator $\tilde{\theta}^{\dagger}_{0,j,\uparrow} = \tilde{c}^{\dagger}_{j,\uparrow}(1-\tilde{n}_{j,\downarrow})$ reads

$$\tilde{\theta}^{\dagger}_{0,j,\uparrow} = \tilde{c}^{\dagger}_{j,\uparrow}(1-\tilde{n}_{j,\downarrow}) = \mathrm{e}^{-\mathrm{i}j\Delta P_J}\frac{\sqrt{n/2}}{G_C} f^{\dagger}_{x_1,s2} f_{x_{j'+1},s1} f_{x_{j'},s1} f^{\dagger}_{x_j,c0}, \tag{18}$$

where the values of the phase-factor momentum $\Delta P_J$ and $U/t$ independent real positive constant $G_C$ are specific to the subspace and are given in [9], the effective $s1$ lattice index reads $j' = jn/2$ and the effective $s2$ lattice is reduced to a single site such that $x_1 = x_j$. Here and below the equality $j' = jn/2$ (and $j' = j\delta$ for the effective $c1$ lattice) should be understood as $j'$ being the closest integer number to $jn/2$ (and $j\delta$). (We recall that the effective $c0$ lattice index $j$ equals that of the rotated-electron lattice [17].)

Next, we consider the excitation $c_{j,\downarrow}|GS\rangle$. Again, more than 99% of the spectral weight corresponds to the excitation $\tilde{\theta}_{0,j,\downarrow}|GS\rangle$. Such an excitation is associated with $\{L_{c,-1/2}, L_{s,-1/2}\} = \{0,0\}$ CPHS ensemble subspaces where according to equation (16), $\tilde{\theta}_{0,j,\downarrow}|GS\rangle = \tilde{c}_{j,\downarrow}(1-\tilde{n}_{j,\uparrow})|GS\rangle$. Here the projector $(1-\tilde{n}_{j,\uparrow})$ is associated with the ground-state lack of rotated-electron double occupation [13]. Most of the spectral weight of this excitation is generated by transitions to the states which span the set of CPHS ensemble subspaces such that

$$\Delta N_{c0} = -1, \qquad \Delta N_{s1} = -1 - 2N_{s2}, \qquad N_{s2} = 0, 1, \tag{19}$$

and $\Delta N^h_{s1} = 1 + 2N_{s2}$. Up to 98% of the spectral weight of $\tilde{\theta}_{0,j,\downarrow}|GS\rangle = \tilde{c}_{j,\downarrow}(1-\tilde{n}_{j,\uparrow})|GS\rangle$ corresponds to the CPHS ensemble subspace whose deviations read $\Delta N_{c0} = -1$, $\Delta N_{s1} = -1$, $N_{s2} = 0$, and $\Delta N^h_{s1} = 1$. These values obey the relation (6). The pseudofermion expression of the operator $\tilde{\theta}_{0,j,\downarrow} = \tilde{c}_{j,\downarrow}(1-\tilde{n}_{j,\uparrow})$ in this subspace is given in equation (46) of [9]. Nearly the whole of the remaining spectral weight of the above electron-removal excitation is associated with the CPHS ensemble subspace whose numbers read $\Delta N_{c0} = -1$, $\Delta N_{s1} = -3$, $N_{s2} = 1$, and $\Delta N^h_{s1} = 3$. These do not obey the relation (6). In this subspace the pseudofermion expression of the operator $\tilde{\theta}_{0,j,\downarrow} = \tilde{c}_{j,\downarrow}(1-\tilde{n}_{j,\uparrow})$ is given by

$$\tilde{\theta}_{0,j,\downarrow} = \mathrm{e}^{-\mathrm{i}j\Delta P_J}\frac{n}{2G_C} f^{\dagger}_{x_1,s2} f_{x_{j'+2},s1} f_{x_{j'+1},s1} f_{x_{j'},s1} f_{x_j,c0}, \tag{20}$$

where $j' = jn/2$ and $x_1 = x_j$.

For the $M_{c,-1/2} = 1$ UHB excitations, let us start by considering electronic densities such that $0 < \delta \leqslant 1$, where $\delta = [1-n]$ is the doping concentration. We are assuming that $\delta$ can be small, but not vanishing. The case of vanishing doping concentrations corresponds to the Mott–Hubbard insulator phase where $(N_a - N^0) = 0$ and to the *doped Mott–Hubbard insulator* such that $(N_a - N^0)$ is finite and will be addressed in the ensuing section. For finite doping concentrations the whole UHB spectral weight of the excitation $\tilde{\theta}^{\dagger}_{0,j,\uparrow}|GS\rangle$ corresponds

to $\{L_{c,-1/2}, L_{s,-1/2}\} = \{0, 0\}$ CPHS ensemble subspaces. According to equation (16), such an excitation can be written as $\tilde{\theta}^{\dagger}_{0,j,\uparrow}|GS\rangle = \tilde{c}^{\dagger}_{j,\uparrow}\tilde{n}_{j,\downarrow}|GS\rangle$ where $\tilde{n}_{j,\downarrow}$ is the UHB projector. For finite values of $\delta$, most of the spectral weight of this excitation is generated by transitions to the excited energy eigenstates which span the set of CPHS ensemble subspaces such that

$$\Delta N_{c0} = -1, \qquad \Delta N_{s1} = -1 - 2N_{s2}, \qquad N_{c1} = 1, \qquad N_{s2} = 0, 1. \tag{21}$$

The deviation in the number of $s1$ pseudofermion holes of these subspaces is $\Delta N^{h}_{s1} = 1+2N_{s2}$. At least 94% of the spectral weight of the excitation $\tilde{\theta}^{\dagger}_{0,j,\uparrow}|GS\rangle = \tilde{c}^{\dagger}_{j,\uparrow}\tilde{n}_{j,\downarrow}|GS\rangle$ corresponds to the CPHS ensemble subspace such that $\Delta N_{c0} = -1$, $\Delta N_{s1} = -1$, $N_{c1} = 1$, $N_{s2} = 0$, and $\Delta N^{h}_{s1} = 1$. These obey the relation (6). In this subspace, the pseudofermion expression of the operator $\tilde{\theta}^{\dagger}_{0,j,\uparrow} = \tilde{c}^{\dagger}_{j,\uparrow}\tilde{n}_{j,\downarrow}$ is given by

$$\tilde{\theta}^{\dagger}_{0,j,\uparrow} = \tilde{c}^{\dagger}_{j,\uparrow}\tilde{n}_{j,\downarrow} = \mathrm{e}^{-\mathrm{i}j\Delta P_J} f^{\dagger}_{x_{j''},c1} f_{x_j,c0} f_{x_{j'},s1}, \tag{22}$$

where $j' = jn/2$ and $j'' = j\delta$. Nearly the whole of the remaining spectral weight of the above UHB excitation is associated with the CPHS ensemble subspace whose numbers are $\Delta N_{c0} = -1$, $\Delta N_{s1} = -3$, $N_{c1} = 1$, $N_{s2} = 1$, and $\Delta N^{h}_{s1} = 3$. These however do not obey the relation (6). In this subspace the pseudofermion expression of the operator $\tilde{\theta}^{\dagger}_{0,j,\uparrow} = \tilde{c}^{\dagger}_{j,\uparrow}\tilde{n}_{j,\downarrow}$ is given by

$$\tilde{\theta}^{\dagger}_{0,j,\uparrow} = \mathrm{e}^{-\mathrm{i}j\Delta P_J}\frac{n}{2G_C} f^{\dagger}_{x_1,s2} f^{\dagger}_{x_{j''},c1} f_{x_{j'+2},s1} f_{x_{j'+1},s1} f_{x_{j'},s1} f_{x_j,c0}, \tag{23}$$

where $j' = jn/2$, $j'' = j\delta$, and $x_1 = x_j$.

## 4. The metal–Mott–Hubbard insulator quantum phase transition

The further understanding of the microscopic processes behind the quantum phase transitions is a problem of great physical interest, as mentioned in section 1. For the 1D Hubbard model there is only one quantum phase transition as a function of the on-site repulsion $U$, which occurs at $U = 0$ for half filling. As a function of the interaction, such transitions are controlled by the dependence on that interaction of the local quantum entanglement [14]. On the other hand for all finite values of $U$ there is a metal–insulator quantum phase transition which occurs as a function of the electronic density at $n = 1$. In terms of the doping that quantum phase transition occurs at $\delta = 0$. Here we study the microscopic effects of that quantum phase transition on the one-electron spectral properties.

Let us consider the case when $\delta$ is vanishing, i.e. there are no $c0$ pseudofermion holes (half-filling) or there is a finite number of such holes in the initial ground state (doped Mott–Hubbard insulator). As the number of holes decreases and one reaches the doped Mott–Hubbard insulator regimen, there arises a competition of the UHB processes considered in the previous section with other UHB processes. The latter processes correspond to the excitation $\tilde{\theta}^{\dagger}_{0,j,\uparrow}|GS\rangle$ for CPHS ensemble subspaces such that $\{L_{c,-1/2}, L_{s,-1/2}\} = \{1, 0\}$. Thus, according to equation (16), one has that $\tilde{\theta}^{\dagger}_{0,j,\uparrow}|GS\rangle = -[(-1)^j/\sqrt{N_a - N^0 + 1}]\tilde{c}^{\dagger}_{j,\downarrow}\tilde{n}_{j,\uparrow}|GS\rangle$, where $\tilde{n}_{j,\uparrow}$ is the UHB projector. Note that for finite values of the doping concentration $\delta$ the one-electron spectral weight associated with such an excitation vanishes in the thermodynamic limit $L \to \infty$. Most of this weight is generated by transitions to the excited energy eigenstates which span the set of CPHS ensemble subspaces such that

$$\Delta N_{c0} = -1, \qquad \Delta N_{s1} = -1 - 2N_{s2}, \qquad L_{c,-1/2} = 1, \qquad N_{s2} = 0, 1, \tag{24}$$

and $\Delta N^{h}_{s1} = 1 + 2N_{s2}$. For vanishing values of the doping concentration at least 94% of the spectral weight of the excitation $\tilde{\theta}^{\dagger}_{0,j,\uparrow}|GS\rangle$ corresponds to the CPHS ensemble subspace with

numbers $\Delta N_{c0} = -1$, $\Delta N_{s1} = -1$, $L_{c,-1/2} = 1$, $N_{s2} = 0$, and $\Delta N^h_{s1} = 1$. Such numbers obey the relation (6). In this subspace the pseudofermion expression of the operator $\tilde{\theta}^{\dagger}_{0,j,\uparrow}$ reads

$$\tilde{\theta}^{\dagger}_{0,j,\uparrow} = -\frac{(-1)^j}{\sqrt{N_a - N^0 + 1}}\tilde{c}^{\dagger}_{j,\downarrow}\tilde{n}_{j,\uparrow} = -\frac{e^{-ij[\Delta P_J + \pi]}}{\sqrt{N_a - N^0 + 1}} f_{x_{j'},s1} f_{x_j,c0}, \tag{25}$$

where $j' = j/2$. Nearly the whole of the remaining spectral weight of such a UHB excitation is associated with the CPHS ensemble subspace whose numbers are $\Delta N_{c0} = -1$, $\Delta N_{s1} = -3$, $L_{c,-1/2} = 1$, and $\Delta N^h_{s1} = 3$. These do not obey the relation (6). In this subspace the pseudofermion expression of the operator $\tilde{\theta}^{\dagger}_{0,j,\uparrow}$ is given by

$$\begin{aligned}\tilde{\theta}^{\dagger}_{0,j,\uparrow} &= -\frac{(-1)^j}{\sqrt{N_a - N^0 + 1}}\tilde{c}^{\dagger}_{j,\downarrow}\tilde{n}_{j,\uparrow} \\ &= \frac{e^{-ij[\Delta P_J + \pi]}}{2G_C\sqrt{N_a - N^0 + 1}} f^{\dagger}_{x_1,s2} f_{x_{j'+2},s1} f_{x_{j'+1},s1} f_{x_{j'},s1} f_{x_j,c0},\end{aligned} \tag{26}$$

where $j' = j/2$ and $x_1 = x_j$.

For finite values of $\delta$, the UHB processes associated with CPHS ensemble subspaces such that $\{L_{c,-1/2}, L_{s,-1/2}\} = \{1, 0\}$ are allowed. However, for finite doping concentrations the relative UHB weight of the $\{L_{c,-1/2}, L_{s,-1/2}\} = \{0, 0\}$ and $\{L_{c,-1/2}, L_{s,-1/2}\} = \{1, 0\}$ processes is approximately given by $1/\delta L$ and thus vanishes in the thermodynamic limit, as mentioned above. Therefore, the weight of the UHB $\{L_{c,-1/2}, L_{s,-1/2}\} = \{1, 0\}$ processes associated with the CPHS ensemble subspaces of numbers (24) vanishes for finite values of $\delta$.

In contrast, for half filling only the UHB $\{1, 0\}$ processes contribute, whereas for finite yet small values of $(N_a - N^0)$ both the $\{0, 0\}$ and $\{1, 0\}$ processes contribute to the UHB spectral weight. If the value of $(N_a - N^0)$ further increases so that $\delta$ becomes finite, the weight of the UHB $\{1, 0\}$ processes vanishes. For $N^0 \neq N_a$ and $(N_a - N^0)$ finite but small, the relative weight of the $\{0, 0\}$ and $\{1, 0\}$ processes is approximately given by $1/[N_a - N^0 + 1]$.

We thus conclude that the collapse of the LHB processes and the interplay between the $\{0, 0\}$ and $\{1, 0\}$ UHB processes for decreasing values of $(N_a - N^0)$ are the main effects of the $(N_a - N^0) \to 0$ metal–Mott–Hubbard insulator quantum phase transition onto the one-electron spectral properties. The ground-state–excited-energy-eigenstate transitions associated with the $\{0, 0\}$ and $\{1, 0\}$ UHB processes change the value of $\eta$ spin by $\Delta\eta = -1/2$ and $\Delta\eta = +1/2$, respectively. For the metallic phase at finite values of the doping concentration the whole UHB weight corresponds to excited states with deviation $\Delta\eta = -1/2$, whereas for the Mott–Hubbard insulator phase only the excited states with deviation $\Delta\eta = +1/2$ are allowed. However, the physics of the doped Mott–Hubbard insulator, which corresponds to a finite number of holes $(N_a - N^0)$, is different: it involves a competition between the two above classes of states. Such a competition is mainly controlled by the form of the operators given in equations (22) and (25), which generate excited energy eigenstates with $\eta$-spin deviations $\Delta\eta = -1/2$ and $\Delta\eta = +1/2$, respectively.

## 5. Concluding remarks

In this paper we used pseudofermion description in the study of the non-perturbative microscopic processes that control the unusual one-electron spectral-weight distributions of the 1D Hubbard model. While at low energy, that model belongs to the universality class of the Luttinger liquid [24], its finite-energy properties are controlled by pseudofermion scattering [10]. Our results are useful for the further understanding and description of the

microscopic mechanisms behind the unusual finite-energy spectral properties observed in quasi-1D compounds [1, 2]. They also provide new insights about the microscopic mechanisms of quantum phase transitions in electronic correlated problems. We found that for the doped Mott–Hubbard insulator there is a competition between the microscopic processes which determine the UHB one-electron spectral distributions of the Mott–Hubbard insulator phase and metallic phase for finite values of the doping concentration. Our studies considered the 1D Hubbard model, which describes successfully some of the exotic properties observed in low-dimensional materials [1–4, 25]. Our results also apply to the related integrable interacting problems [26] and therefore have wide applicability.

## Acknowledgments

We thank Daniel Bozi, Ralph Claessen, Patrick A Lee, Tiago C Ribeiro, and Pedro D Sacramento for stimulating discussions and the support of the ESF Science Programme INSTANS 2005-2010. JMPC thanks the MIT for hospitality and support and the Gulbenkian Foundation, Fulbright Commission, and FCT under the grant POCTI/FIS/58133/2004 for financial support, and KP acknowledges the support of the OTKA grant T049607.

## References

[1] Carmelo J M P, Penc K, Martelo L M, Sacramento P D, Lopes dos Santos J M B, Claessen R, Sing M and Schwingenschlögl U 2004 *Europhys. Lett.* **67** 233
Carmelo J M P, Bozi D, Sacramento P D and Penc K 2005 submitted
[2] Sing M, Schwingenschlögl U, Claessen R, Blaha P, Carmelo J M P, Martelo L M, Sacramento P D, Dressel M and Jacobsen C S 2003 *Phys. Rev.* B **68** 125111
[3] Benthien H, Gebhard F and Jeckelmann E 2004 *Phys. Rev. Lett.* **92** 256401
[4] Carmelo J M P, Guinea F, Penc K and Sacramento P D 2004 *Europhys. Lett.* **68** 839
[5] Simons B D, Lee P A and Altshuler B L 1993 *Phys. Rev. Lett.* **70** 4122
Penc K and Shastry B S 2002 *Phys. Rev.* B **65** 155110
[6] Lieb Elliott H and Wu F Y 1968 *Phys. Rev. Lett.* **20** 1445
Ramos P B and Martins M J 1997 *J. Phys. A: Math. Gen.* **30** L195
[7] Takahashi M 1972 *Prog. Theor. Phys.* **47** 69
[8] Carmelo J M P, Penc K and Bozi D 2005 *Nucl. Phys.* B **725** 421
Carmelo J M P and Penc K 2006 *Nucl. Phys.* B **737** 237
Carmelo J M P and Penc K 2006 *Nucl. Phys.* B **737** 351 (erratum)
[9] Carmelo J M P and Penc K 2003 *Preprint* cond-mat/0311075
[10] Carmelo J M P 2005 *J. Phys.: Condens. Matter* **17** 5517
[11] Penc K, Hallberg K, Mila F and Shiba H 1996 *Phys. Rev. Lett.* **77** 1390
[12] Penc K, Hallberg K, Mila F and Shiba H 1997 *Phys. Rev.* B **55** 15475
[13] Carmelo J M P, Román J M and Penc K 2004 *Nucl. Phys.* B **683** 387
[14] Gu S J, Deng S S, Li Y Q and Lin H Q 2004 *Phys. Rev. Lett.* **93** 086402
[15] Heilmann O J and Lieb E H 1971 *Ann. New York Acad. Sci.* **172** 583
[16] Yang C N 1989 *Phys. Rev. Lett.* **63** 2144
[17] Carmelo J M P 2005 *Preprint* cond-mat/0508141
[18] Mizuno Y, Tsutsui K, Tohyama T and Maekawa S 2000 *Phys. Rev.* B **62** R4769
[19] MacDonald A H, Girvin S M and Yoshioka D 1988 *Phys. Rev.* B **37** 9753
[20] Takahashi M 1977 *J. Phys. C: Solid State Phys.* **10** 1289
[21] Sorella S and ans Parola A 1998 *Phys. Rev.* B **57** 6444
[22] Talstra J C, Strong S P and Anderson P W 1995 *Phys. Rev. Lett.* **74** 5256
Talstra J C and Strong S P 1997 *Phys. Rev.* B **56** 6094
[23] Joynt R 2000 *Science* **284** 777
[24] Carmelo J M P, Castro Neto A H and Campbell D K 1994 *Phys. Rev. Lett.* **73** 926
Carmelo J M P, Castro Neto A H and Campbell D K 1995 *Phys. Rev. Lett.* **74** 3089 (erratum)
Carmelo J M P, Castro Neto A H and Campbell D K 1994 *Phys. Rev.* B **50** 3683
[25] Baeriswyl D, Carmelo J and Maki K 1987 *Synth. Met.* **21** 271
Carmelo J M P, Horsch P, Campbell D K and Castro Neto A H 1993 *Phys. Rev.* B **48** 4200 (RC)
Peres N M R, Carmelo J M P, Campbell D K and Sandvik A W 1997 *Z. Phys.* B **103** 217
[26] Bares P A, Carmelo J M P, Ferrer J and Horsch P 1992 *Phys. Rev.* B **46** 14624